

Determination of B_K using improved staggered fermions (I): SU(3) chiral perturbation theory fit

Taegil Bae*, Hyung-Jin Kim, Jangho Kim, Jongjeong Kim, Kwangwoo Kim, Boram Yoon, Weonjong Lee

Frontier Physics Research Division and Center for Theoretical Physics

Department of Physics and Astronomy, Seoul National University, Seoul, 151-747, South Korea

E-mail: wlee@snu.ac.kr

Chulwoo Jung

Physics Department, Brookhaven National Laboratory, Upton, NY11973, USA

E-mail: chulwoo@bnl.gov

Stephen R. Sharpe

Physics Department, University of Washington, Seattle, WA 98195-1560

E-mail: sharpe@phys.washington.edu

We present the results for B_K calculated using HYP-smearred staggered fermions using lattices generated by the MILC collaboration using the asqtad staggered action. We have done the calculation on 8 ensembles of these lattices, including three different lattice spacings ($a = 0.12, 0.09, 0.06$ fm). We fit the data to forms based on those predicted by SU(3) mixed-action partially-quenched staggered chiral perturbation theory. Our preliminary result is $B_K(\text{NDR}, \mu = 2 \text{ GeV}) = 0.528 \pm 0.010 \pm 0.040$, where the first error is statistical and the second systematic. The error turns out to be larger than that from an analysis using SU(2) chiral perturbation theory.

*The XXVII International Symposium on Lattice Field Theory - LAT2009
July 26-31 2009 Peking University, Beijing, China*

*Speaker.

1. Introduction

Indirect CP violation in the neutral kaon system and is conventionally parameterized by $\varepsilon = (2.228 \pm 0.011) \times 10^{-3}$. In the Standard Model, this experimental parameter is related to the matrix element of a $\Delta S = 2$ four-fermion operator, itself parameterized by

$$B_K = \frac{\langle K_0 | \bar{s} \gamma_\mu^L d \bar{s} \gamma_\mu^L d | K_0 \rangle}{(8/3) f_K^2 M_K^2}. \quad (1.1)$$

The relation between experiment and theory takes the form (see, e.g., Ref. [1, 2])

$$\varepsilon = \exp(i\phi_\varepsilon) \sin(\phi_\varepsilon) \left[\sqrt{2} C_\varepsilon \text{Im} \lambda_t X \hat{B}_K + \xi \right] + \text{dim-8 contributions}, \quad (1.2)$$

where ϕ_ε is the (well-determined) phase of ε_K ,

$$C_\varepsilon = \frac{G_F^2 F_K^2 m_K M_W^2}{6\sqrt{2}\pi^2 \Delta M_K}, \quad \lambda_i = V_{is}^* V_{id}, \quad (1.3)$$

and the dependence on charm and top masses enters through the Inami-Lin functions $S_{0,3}$

$$X = \text{Re} \lambda_c [\eta_1 S_0(x_c) - \eta_3 S_3(x_c, x_t)] - \text{Re} \lambda_t \eta_2 S_0(x_t), \quad x_i = m_i^2 / M_W^2, \quad (1.4)$$

with η_{1-3} Wilson coefficients. The $\xi = \text{Im} A_0 / \text{Re} A_0$ term in (1.2) provides a small correction to the proportionality of ε_K and B_K , one that must be included now that results for B_K have errors below the 10% level [2]. For completeness we note that the contributions of operators of dimension-8 have been estimated to be very small, enhancing B_K by $\sim 0.5\%$ [5].

An accurate determination of B_K thus constrains the CKM matrix, as discussed here in the review of Van de Water [3]. Several groups are pursuing this calculation, using a variety of lattice fermions [4]. Since chiral symmetry constrains the four-fermion matrix element, lattice fermions with some measure of chiral symmetry are preferred. Our approach is to use improved staggered fermions, which are computationally cheap, although one pays some price due to taste-breaking effects. More precisely we use HYP-smearred valence staggered fermions (since HYP-smearing is effective at reducing taste-breaking) and asqtad staggered sea quarks (i.e. the MILC ensembles). We take advantage of the exact $U(1)_A$ chiral symmetry and control the systematic errors due to the taste symmetry breaking using staggered chiral perturbation theory (SChPT) [6, 7, 8].

This paper is the first report in a series of the four describing different aspects of our work. Here we explain briefly the fitting procedures and results from our $SU(3)$ SChPT analysis.

2. $SU(3)$ Staggered ChPT Analysis

In setting up a calculation of B_K using staggered fermions, one must deal with the additional taste degree of freedom. For the sea-quarks, this is done by using a rooted determinant. For the valence quarks, one must choose a particular taste for the external kaons, and choose the lattice operator so as to match the matrix element onto the desired continuum one. Away from the continuum limit, there are then several sources of error: taste-symmetry breaking coupled with rooting leads to unphysical (unitarity violating) effects; taste-symmetry breaking in the valence sector leads to

significant changes to the size of chiral logarithms; and approximate matching of the lattice and continuum matrix elements (in our case using one-loop perturbation theory) leads to truncation errors proportional to powers of α . All these effects are incorporated into SChPT, which thus provides a method to systematically control and remove these sources of error. It has been applied successfully to the analysis of the π , K , D and B meson masses and decay constants, as reviewed in Ref. [9].

The theoretical SChPT analysis was generalized to B_K in Ref. [8], and the result worked out to next-to-leading order (NLO). This work assumed the same staggered action for both valence and sea quarks and thus is not directly applicable to our mixed-action setup. We have carried out the appropriate generalization, as summarized in Ref. [10]. Full details will be presented in Ref. [11].

The power-counting used in the SChPT calculation is $m_q/\Lambda_{\text{QCD}} \sim (a\Lambda_{\text{QCD}})^2 \sim \alpha/\pi \sim \alpha^2$. Discretization errors proportional to a^2 and to $a^2\alpha^2$ are treated as of the same size, since, in practice, the latter (which include taste-breaking effects) are numerically enhanced. Since the dominant one-loop matching contributions are included, and the coefficients of the taste-breaking operators known to be small, these residual one-loop effects (denoted α/π above) are treated as comparable to the unknown two-loop effects (α^2 above). For more discussion see Ref. [8].

In the $SU(3)$ SChPT analysis m_q can be the mass of the light or strange sea-quarks (m_ℓ and m_s , respectively), or the mass of the down or strange valence quark (m_x and m_y , respectively). An important issue is whether m_s/Λ_{QCD} and m_y/Λ_{QCD} are small enough for NLO ChPT to be useful. We address this phenomenologically by including an analytic NNLO term.

At fixed a , the NLO expression contains 15 different low-energy coefficients (LECs).¹ 4 of these are present in the continuum, while the remaining 11 arise from taste-violating discretization and truncation errors (including 2 which are introduced by the use of a mixed action). Although we calculate B_K for 55 different combinations of m_x and m_y , and in some cases for several values of m_ℓ , it is not possible to do an unconstrained fit to the full functional form. This is partly because the functions fall into groups within which they are very similar (differing, for example, by the taste of the pion in the loops). The differences within groups are comparable to or smaller than our statistical errors. We have chosen to proceed by picking one of functions from each group as a representative. In addition, as described in Ref. [10], the success of HYP smearing at reducing taste breaking implies that two of the LECs are very small, and so we have dropped these terms.

After these choices, the number of parameters associated with taste-breaking is reduced from 11 to 3, so the total number is reduced to the more manageable 7. We write the fitting function as:

$$f_{\text{th}} = \sum_{i=1}^7 c_i F_i \quad (2.1)$$

where c_i are the coefficients (related to SChPT LECs), while the functions are

$$F_1 = 1 + \frac{1}{8\pi^2 f_\pi^2 G} [M_{\text{conn}} + M_{\text{disc}}], \quad F_2 = G/\Lambda^2, \quad F_3 = (G/\Lambda^2)^2, \quad F_4 = F_T^{(4)} \quad (2.2)$$

$$F_5 = \frac{(X_P - Y_P)^2}{G\Lambda^2}, \quad F_6 = F_{\text{VA}}^{(6)}, \quad F_7 = F_A^{(1)}, \quad (2.3)$$

¹Not including f_π , which we fix at its experimental value, taking the scale from the MILC collaboration.

and depend on the various pseudo-Goldstone boson (PGB) masses. Our notation is that $G \equiv K_P$ is the squared mass of the taste- ξ_5 valence PGB with flavor composition xy , X_B and Y_B are the squared masses of the taste-B valence PGBs with compositions xx and yy , respectively, and $\Lambda_\chi \approx 4\pi f_\pi$ is the ChPT scale. We set $\Lambda_\chi = 1$ GeV in our fits—changing this value results in shifts in the LECs.

The function F_1 contains the continuum-like chiral logarithms, with discretization errors entering through the taste-breaking in the masses of the PGBs in the loops. The quark-line connected part is:

$$M_{\text{conn}} = \sum_{B=I,P,V,A,T} \frac{\tau^B}{2} \left[(G + X_B)\ell(X_B) + (G + Y_B)\ell(Y_B) + 2(G - K_B)\ell(K_B) - 2GK_B\tilde{\ell}(K_B) \right] \quad (2.4)$$

where τ^B is the fractional multiplicity of taste B, and the chiral logarithmic functions are

$$\ell(X) = X \log(X/\mu_{\text{DR}}^2), \quad \tilde{\ell}(X) = -\frac{d\ell(X)}{dX} = -\log(X/\mu_{\text{DR}}^2) - 1, \quad (2.5)$$

up to (known) finite-volume corrections. The expression for the quark-line disconnected part M_{disc} is more lengthy: it can be deduced from the results in Ref. [8] and will be given in Ref. [11]. The important point is that, like M_{conn} it is fully predicted in terms of f_π and PGB masses that can be calculated in our simulation or obtained from the results of the MILC collaboration.

The analytic terms F_2 and F_5 are also present in the continuum, as is the NNLO analytic term F_3 . Note that F_5 vanishes when $m_x = m_y$.

The remaining three terms are due to taste-breaking discretization or truncation errors, and are thus pure lattice artefacts. Of the three, only F_4 is non-vanishing when $m_x = m_y$. For brevity, we show only the two simplest functions:

$$F_T^{(4)} = \frac{3}{8} \frac{1}{f_\pi^2 G} \left\{ 2G\tilde{\ell}(K_T) + [\ell(X_T) + \ell(Y_T) - 2\ell(K_T)] \right\}, \quad (2.6)$$

$$F_{VA}^{(6)} = \frac{3}{8} \frac{1}{f_\pi^2 G} \left\{ [\ell(X_T) + \ell(Y_T) - 2\ell(K_T)] \right\}, \quad (2.7)$$

$F_A^{(1)}$ can be deduced from Ref. [8] and will be given in Ref. [11].

3. Fitting procedure

We calculate B_K using standard methods [12] on the MILC lattices listed in Table 1. We use the 10 valence quark masses given in Table 2, and thus have 55 different mass combinations for the PGBs: 10 degenerate and 45 non-degenerate. We use one-loop matching.

We use several fitting procedures, but focus here on the one used for our central value. In this fit we do not yet include the finite-volume corrections predicted by ChPT. First, we fit the degenerate data. The general form (2.1) reduces to $\sum_{i=1}^4 c_i F_i$ in the degenerate limit. We know the expected size of each term; in particular, we expect c_4 to have the magnitude $c_4 \approx a^2 \Lambda_{\text{QCD}}^4$ if it is dominated by discretization errors. We implement this prior knowledge using Bayesian fitting [13] in which the standard χ^2 is augmented by the addition of

$$\chi_{\text{prior}}^2 = \frac{(c_4 - a_4)^2}{\tilde{\sigma}_4^2}. \quad (3.1)$$

a (fm)	am_l/am_s	geometry	ens \times meas	ID
0.12	0.03/0.05	$20^3 \times 64$	564×1	C1
0.12	0.02/0.05	$20^3 \times 64$	486×1	C2
0.12	0.01/0.05	$20^3 \times 64$	671×9	C3
0.12	0.01/0.05	$28^3 \times 64$	274×8	C3-2
0.12	0.007/0.05	$20^3 \times 64$	651×1	C4
0.12	0.005/0.05	$24^3 \times 64$	509×1	C5
0.09	0.0062/0.031	$28^3 \times 96$	995×1	F1
0.06	0.0036/0.018	$48^3 \times 144$	513×1	S1

Table 1: MILC lattices used for the numerical study. Here “ens” and “meas” are the number of gauge configurations and measurements per configuration, respectively, and “ID” is a label.

a (fm)	am_x and am_y	n
0.12	$0.005 \times n$	1, 2, 3, ..., 10
0.09	$0.003 \times n$	1, 2, 3, ..., 10
0.06	$0.0018 \times n$	1, 2, 3, ..., 10

Table 2: Valence quark masses used for the numerical study (with $m_x \leq m_y$).

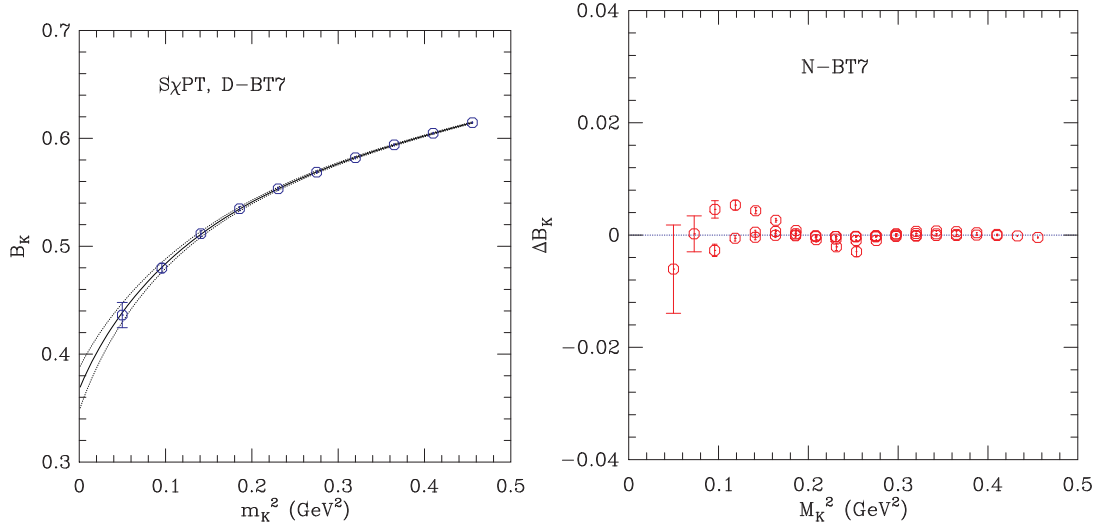


Figure 1: B_K vs. m_K^2 (left) and ΔB_K vs. m_K^2 (right): The results are on the C3 lattices. The fit types are D-BT7 (left, degenerate case) and N-BT7 (right, non-degenerate case).

We take $a_4 = 0$ since we do not know the sign of c_4 , and $\tilde{\sigma}_4 = a^2 \Lambda_{\text{QCD}}^4$ with $\Lambda_{\text{QCD}} = 0.3 \text{ GeV}$. Minimizing the augmented χ^2 leads to the fit we label D-BT7 (with “D” for degenerate).² An example is shown in the left panel of Fig. 1.

Next we fit f_{th} to all 55 data points, but using the results for c_{1-4} and their errors from the D-BT7 fit as priors for the first four parameters. We also include priors for the coefficients c_6 and

²At the present stage, our χ^2 includes only the diagonal elements of the correlation matrix.

c_7 , whose expected magnitudes are $c_6 \approx c_4$ and $c_7 \approx \Lambda_{\text{QCD}}^2 c_4$. In total then, χ^2 is augmented by

$$\sum_{i=1}^4 \frac{(c_i - a_i)^2}{\tilde{\sigma}_i^2} + \sum_{i=6,7} \frac{(c_i - a_i)^2}{\tilde{\sigma}_i^2} \quad (3.2)$$

with a_{1-4} set to the central values of c_{1-4} from the D-BT7 fit, and $\tilde{\sigma}_{1-4}$ set to the corresponding errors, while $a_6 = a_7 = 0$, $\tilde{\sigma}_6 = a^2 \Lambda_{\text{QCD}}^4$ and $\tilde{\sigma}_7 = a^2 \Lambda_{\text{QCD}}^6$. The resulting fit is labeled N-BT7 (“N” for non-degenerate). An example is shown in the right panel of Fig. 1, where ΔB_K is the residual:

$$\Delta B_K \equiv B_K(\text{data}) - f_{\text{th}}. \quad (3.3)$$

The fit works well except for the non-degenerate points in which m_x takes its smallest value, which we suspect is due in part due to finite-volume effects.

We have tried many variations of this fitting strategy: relaxing the constraints on $c_{4,6,7}$ to the values one might expect if $O(\alpha^2)$ [rather than $O(a^2)$] effects were dominant (type N-BT7-2); fitting in one stage to all data-points with either $O(a^2)$ or $O(\alpha^2)$ priors on $c_{4,6,7}$ (types N-BT8 and N-BT8-2); and simply fitting without priors (N-T2). The results for the continuum-like parameters c_{1-3} and c_5 are consistent between fits, while those for the lattice artefacts c_4 , c_{6-7} vary significantly. An intriguing result is that we find c_5 to be remarkably smaller than the expected size [$c_5 \sim O(1)$].

For each fit, we determine a value for B_K at the physical valence-quark masses by setting all lattice artefacts to zero in the SChPT expression. We can then attempt to extrapolate to the continuum and infinite volume limits, and to the physical values of m_ℓ and m_s . Examples of some of these extrapolations are shown in the companion proceedings [14, 15, 16].

4. Error budget and conclusion

source	error (%)	description
statistics	2.0	N-BT7 fit
discretization	2.5	diff. of (S1) and ($a = 0$)
fitting (1)	0.6	diff. of N-BT7 and N-BT8 (C3)
fitting (2)	5.4	diff. of N-BT7 and N-BT7-2 (C3)
fitting (3)	1.3	fit w.r.t. am_l
finite volume	2.2	diff. of C3 and C3-2
matching factor	3.6	$\Delta B_K^{(2)}$ (S1)
scale r_1	0.07	uncertainty in r_1

Table 3: Preliminary error budget for B_K obtained using $SU(3)$ SChPT fitting.

In Table 3, we summarize our present best estimates of the uncertainties in B_K coming from various sources. These are conservative estimates, some of which may decrease with further analysis. The method by which we estimate these errors is outlined in the “description”. The first fitting error estimates the (rather small) impact of fitting in two stages rather than in one, while the second fitting error estimates the impact of changing the widths $\tilde{\sigma}_{4,6,7}$ for the priors. The latter error is our dominant systematic—it indicates that we cannot pin down the functional form of B_K well enough

to extrapolate to the physical light-quark mass with less than 5% uncertainty (at least on the coarse lattices).

Our current, **preliminary** estimate of B_K using $SU(3)$ ChPT fitting is

$$B_K(\text{NDR}, \mu = 2 \text{ GeV}) = 0.528 \pm 0.011 \pm 0.040 \quad [\text{SU}(3), \text{PRELIMINARY.}] \quad (4.1)$$

where the first error is statistical and the second combines all systematic errors. This turns out to be less accurate than the results from $SU(2)$ ChPT fitting [14].

5. Acknowledgments

C. Jung is supported by the US DOE under contract DE-AC02-98CH10886. The research of W. Lee is supported by the Creative Research Initiatives Program (3348-20090015) of the NRF grant funded by the Korean government (MEST). The work of S. Sharpe is supported in part by the US DOE grant no. DE-FG02-96ER40956. Computations were carried out in part on facilities of the USQCD Collaboration, which are funded by the Office of Science of the U.S. Department of Energy.

References

- [1] Andrzej J. Buras, [hep-ph/9806471].
- [2] A.J. Buras and D. Guadagnoli, Phys. Rev. D78 (2008) 033005 [arXiv:0805.3887].
- [3] Ruth Van de Water, PoS (LAT2009) 014.
- [4] Victorio Lubicz, PoS (LAT2009) 013.
- [5] O. Cata and S. Peris, JHEP **0407**, 079 (2004) [arXiv:hep-ph/0406094].
- [6] Weonjong Lee and Stephen Sharpe, Phys. Rev. D**60** (1999) 094503, [hep-lat/9905023].
- [7] C. Aubin and C. Bernard, Phys. Rev. D**68** (2003) 034014, [hep-lat/0304014].
- [8] Ruth S. Van de Water, Stephen R. Sharpe, Phys. Rev. D**73** (2006) 014003, [hep-lat/0507012].
- [9] A. Bazavov, *et al.*, MILC Collaboration, [arXiv:0903.3598].
- [10] T. Bae, *et al.*, PoS (Lattice 2008) 275, [arXiv:0809.1220].
- [11] T. Bae, *et al.*, in preparation.
- [12] Weonjong Lee, *et al.*, Phys. Rev. D71 (2005) 094501, [hep-lat/0409047].
- [13] G.P. Lepage, *et al.*, Nucl. Phys. (Proc. Suppl.) B106 (2002) 12, [arXiv:hep-lat/0110175].
- [14] Hyung-Jin Kim, *et al.*, PoS (LAT2009) 262.
- [15] Boram Yoon, *et al.*, Pos (LAT2009) 263.
- [16] Jangho Kim, *et al.*, Pos (LAT2009) 264.